Rashidi, M. M., *et al.*: Numerical Solution for Thermophoresis Effects on Heat and Mass ...
THERMAL SCIENCE: Year 2017, Vol. 21, No. 6B, pp. 2719-2730

2719

NUMERICAL SOLUTION FOR THERMOPHORESIS EFFECTS ON HEAT AND MASS TRANSFER OVER AN ACCELERATING SURFACE WITH HEAT SOURCE/SINK

by

Mohammad Mehdi RASHIDI[a,b], Ramachandran SIVARAJ[c*], Durairaj MYTHILI[c], and Zhigang YANG[a,b]

[a] Shanghai Key Laboratory of Vehicle Aerodynamics and Vehicle Thermal Management Systems, Tongji University, Shanghai, China
[b] ENN-Tongji Clean Energy Institute of Advanced Studies, Shanghai, China
[c] Fluid Dynamics Division, School of Advanced Sciences, VIT University, Vellore, India

A study has been carried out to analyze the thermophoretic particle deposition and heat generation/absorption effects on unsteady, free convective, viscous fluid flow over a moving flat plate. The thermal conductivity of the fluid is assumed to vary as a linear function of temperature. The governing partial differential equations are solved numerically by using an implicit finite difference method of Crank Nicolson type. Numerical results for the velocity, temperature and concentration profiles as well as for the skin-friction coefficient, Nusselt number and Sherwood number distributions are obtained and presented graphically for various parametric conditions to show interesting aspects of the solution. Results indicate that the heat source/sink plays a vital role in predicting the heat transfer characteristics of moving fluids and the thermophoretic particle deposition has notable influence on the mass transfer characteristics.

Key words: *free convection, heat source/sink, variable thermal conductivity, thermophoresis, moving plate*

Introduction

The theory of laminar boundary-layer flows on a moving surface occurs in several engineering applications. Aerodynamic extrusion of a plastic sheet, the cooling of an infinite metallic plate in a cooling bath and filament extruded continuously from a dye are examples of practical applications. Continuously moving surface through an otherwise quiescent medium has many applications in manufacturing processes. Such processes are hot rolling, wire drawing, spinning of filaments, metal extrusion, crystal growing, continuous casting, glass fiber production, and paper production [1-6].

For the fluids, which are important in the theory of lubrication, the heat generated by the internal friction and the corresponding rise in temperature do affect the thermal conductivity of the fluid. Variable thermal conductivity heat transfer occurs in many engineering applications. Heat transfer in furnaces, boilers, porous burners, volumetric solar receivers, fibrous and foam insulations are some examples of combined conduction and radiation problems in which

---

* Corresponding author, e-mail: sivaraj.kpm@gmail.com

2720

Rashidi, M. M., *et al.*: Numerical Solution for Thermophoresis Effects on Heat and Mass ...
THERMAL SCIENCE: Year 2017, Vol. 21, No. 6B, pp. 2719-2730

the changes of temperature and hence the variations of thermal conductivity are large. Variable thermal conductivity in convective heat transfer problems may be observed in heat exchangers and cooling systems of electronic devices. The assumption of constant thermal conductivity in simulating such cases may result in considerable error [7-11].

The presence of heat generation/absorption may alter the temperature distribution in the fluid which in turn affects the particle deposition rate in systems such as nuclear reactors, electronic chips and semiconductor wafers. The analysis of the temperature field as modified by the generation/absorption of heat in moving fluids is important in view of several physical problems, such as in a chemical reaction taking place and in problems concerned with dissociating fluids. In the literature there are several papers highlighting the importance of temperature dependent heat source/sink on the heat transfer of various fluids. However, they ignored the effects of space dependent heat source/sink which is also important in the heat transfer analysis [12-19].

The deposition of small micron sized particles suspended in a non-isothermal gas from a hot surface towards a cold one due to temperature gradients is known as thermophoretic deposition. In this process, the repulsion of particles from hot objects also takes place and a particle-free layer is observed around hot bodies. The magnitudes of thermophoretic force and velocity are proportional to the temperature gradient and depend on thermal conductivity of aerosol particles, the carrier gas, heat capacity of the gas, thermophoretic coefficient, and Knudsen number. The model finds applications in particles impacting the blade surface of gas turbines, aerosol technology, deposition of silicon thin films and air pollution control. Representative studies in this area can be found in [20-23]. Some recent interesting contributions pertaining to heat transfer aspects are cited in [24-27]. Some similar papers in this field can be found in [28-32].

In view of the previous discussions, authors envisage to investigate the thermophoretic particle deposition and heat generation/absorption effects on unsteady, free convective, viscous fluid flow over a moving flat plate subject to variable thermal conductivity of the fluid. The Crank-Nicolson method is used to solve the coupled non-linear equations of the problem. The results of parametric study on the flow, heat and mass transfer characteristics are shown graphically and the physical aspects are discussed in detail.

Mathematical formulation

Consider a 2-D, unsteady, free convective flow of a viscous fluid over an accelerating flat plate as shown in fig. 1.

The x-axis is taken in the direction along the surface of the plate which is set to motion and the y-axis is taken perpendicular to it. The wall $y = 0$ is maintained at constant temperature, T_w, and concentration, C_w, higher than the ambient temperature, T_∞, and ambient concentration, C_∞, respectively. The fluid is assumed to be incompressible and the accelerating surface issues from a thin slit at the origin. It is assumed that the speed of a point on the plate is proportional to its distance from the slit and boundary-layer approximations are utilized. The heat equation includes the effects of heat source/sink whereas the mass diffusion equation includes the thermophoresis effect. The fluid properties such as density, viscosity and molecular diffusivity are assumed to be constant, except the thermal conductivity which is assumed to be varying as a linear function of tempera-
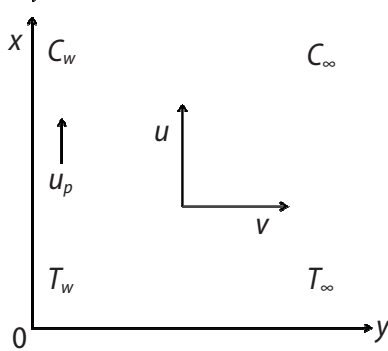

Figure 1. Flow geometry of the problem

Rashidi, M. M., *et al.*: Numerical Solution for Thermophoresis Effects on Heat and Mass ...
THERMAL SCIENCE: Year 2017, Vol. 21, No. 6B, pp. 2719-2730

2721

ture. Taking into consideration of these assumptions, the equations that describe the physical situation can be written in Cartesian frame of references:

$$\frac{\partial u}{\partial x} + \frac{\partial v}{\partial y} = 0 \tag{1}$$

$$\frac{\partial u}{\partial t^*} + u\frac{\partial u}{\partial x} + v\frac{\partial u}{\partial y} = \nu\frac{\partial^2 u}{\partial y^2} \tag{2}$$

$$\frac{\partial T}{\partial t^*} + u\frac{\partial T}{\partial x} + v\frac{\partial T}{\partial y} = \frac{1}{\rho c_p}\frac{\partial}{\partial y}\left(k_f\frac{\partial T}{\partial y}\right) + \frac{\beta u}{\rho c_p}(T_\infty - T) \tag{3}$$

$$\frac{\partial C}{\partial t^*} + u\frac{\partial C}{\partial x} + v\frac{\partial C}{\partial y} + \frac{\partial(C\,V_T)}{\partial y} = D\frac{\partial^2 C}{\partial y^2} \tag{4}$$

The appropriate initial and boundary conditions of the problem are:

$$
\begin{aligned}
t^* \le 0: \quad & u = 0, \quad v = 0, \quad T = T_\infty, \quad C = C_\infty \quad \text{for all} \quad x, y \\
t^* > 0: \quad & u = u_p, \quad v = 0, \quad T = T_w, \quad C = C_w \quad \text{at} \quad y = 0 \\
& u = 0, \quad v = 0, \quad T = T_\infty, \quad C = C_\infty \quad \text{at} \quad x = 0 \\
& u \to 0, \quad T \to T_\infty, \quad C \to C_\infty \quad\quad\quad \text{as} \quad y \to \infty
\end{aligned}
\tag{5}
$$

The variations of thermal conductivity are written in the form [7]:

$$k_f = k_0\left(1 + N\frac{T - T_\infty}{T_w - T_\infty}\right) \tag{6}$$

when the wall temperature, T_w, exceeds the free stream temperature, T_∞, the last term in eq. (3) represents the heat source (when $\beta < 0$) and the heat sink (when $\beta > 0$). For the condition that $T_w < T_\infty$, the opposite relationship is true, $\beta u(T_\infty - T)$ is assumed to be the amount of heat generated/absorbed per unit volume.

The effect of thermophoresis is usually prescribed by means of an average velocity, which a particle will acquire when exposed to a temperature gradient. In boundary-layer flow, the temperature gradient in the y-direction is very much larger than in the x-direction, and therefore only the thermophoretic velocity in y-direction is considered.

The thermophoretic velocity, V_T, can be written [20]:

$$V_T = -\frac{K_T\nu}{T_r}\frac{\partial T}{\partial y} \tag{7}$$

where the thermophoretic coefficient, K_T, ranges in value from 0.2 to 1.2 [21] and is defined:

$$K_T = \frac{2C_s\left(\dfrac{k_0}{k_p} + C_t\,\text{Kn}\right) + 1 + \text{Kn}\left(C_1 + C_2 e^{-C_3/\text{Kn}}\right)}{(1 + 3C_m\,\text{Kn})\left(1 + \dfrac{k_0}{k_p} + 2C_t\,\text{Kn}\right)} \tag{8}$$

Introducing the following non-dimensional quantities:

$$X = \frac{x}{L}, \quad Y = \frac{y}{L}(\text{Gr})^{1/4}, \quad U = \frac{uL}{\nu}(\text{Gr})^{-1/2}, \quad V = \frac{\nu L}{\nu}(\text{Gr})^{-1/4}, \quad t = \frac{\nu t^*}{L^2}(\text{Gr})^{1/2}$$

$$\theta = \frac{T - T_\infty}{T_w - T_\infty}, \quad \phi = \frac{C - C_\infty}{C_w - C_\infty}, \quad \text{Gr} = \frac{g\beta_T(T_w - T_\infty)L^3}{\nu^2}, \quad \text{Pr} = \frac{\mu c_p}{k_0}, \quad \delta = \frac{\beta L}{\rho c_p}, \quad (9)$$

$$\text{Sc} = \frac{\nu}{D}, \quad \tau_T = \frac{-k_0(T_w - T_\infty)}{T_r}, \quad U_P = \frac{Lu_p}{\nu(\text{Gr})^{1/2}}$$

In view of eq. (9), basic field of eqs. (1)-(4) can be expressed in non-dimensional form:

$$\frac{\partial U}{\partial X} + \frac{\partial V}{\partial Y} = 0 \tag{10}$$

$$\frac{\partial U}{\partial t} + U\frac{\partial U}{\partial X} + V\frac{\partial U}{\partial Y} = \frac{\partial^2 U}{\partial Y^2} \tag{11}$$

$$\frac{\partial \theta}{\partial t} + U\frac{\partial \theta}{\partial X} + \left(V - \frac{N}{\text{Pr}}\frac{\partial \theta}{\partial Y}\right)\frac{\partial \theta}{\partial Y} = \left(\frac{1 + N\theta}{\text{Pr}}\right)\frac{\partial^2 \theta}{\partial Y^2} - \delta U\theta \tag{12}$$

$$\frac{\partial \phi}{\partial t} + U\frac{\partial \phi}{\partial X} + \left(V + \tau_T\frac{\partial \theta}{\partial Y}\right)\frac{\partial \phi}{\partial Y} + \tau_T\frac{\partial^2 \theta}{\partial Y^2}\phi = \frac{1}{\text{Sc}}\frac{\partial^2 \phi}{\partial Y^2} \tag{13}$$

The appropriate initial and boundary conditions become:

$$\begin{aligned}
t \leq 0: \quad & U = 0, \quad V = 0, \quad \theta = 0, \quad \phi = 0 \quad \text{for all} \quad X, Y \\
t > 0: \quad & U = U_P, \quad V = 0, \quad \theta = 1, \quad \phi = 1 \quad \text{at} \quad Y = 0 \\
& U = 0, \quad V = 0, \quad \theta = 0, \quad \phi = 0 \quad \text{at} \quad X = 0 \\
& U \to 0, \quad \theta \to 0, \quad \phi \to 0 \qquad \text{as} \quad Y \to \infty
\end{aligned} \tag{14}$$

The dimensionless local values of skin friction, τ, Nusselt number, and Sherwood number can be characterized in order by:

$$\tau = -\left(\frac{\partial U}{\partial Y}\right)_{Y=0}, \quad \text{Nu} = -X\left(\frac{\partial \theta}{\partial Y}\right)_{Y=0}, \quad \text{Sh} = -X\left(\frac{\partial \phi}{\partial Y}\right)_{Y=0} \tag{15}$$

Average skin friction, $\overline{\tau}$, average Nusselt number, $\overline{\text{Nu}}$, and average Sherwood number, $\overline{\text{Sh}}$, in dimensionless form can be written:

$$\overline{\tau} = -\int_0^1 \left(\frac{\partial U}{\partial Y}\right)_{Y=0} dX, \quad \overline{\text{Nu}} = -\int_0^1 \frac{1}{\theta_{Y=0}}\left(\frac{\partial \theta}{\partial Y}\right)_{Y=0} dX, \quad \overline{\text{Sh}} = -\int_0^1 \frac{1}{\phi_{Y=0}}\left(\frac{\partial \phi}{\partial Y}\right)_{Y=0} dX \tag{16}$$

Finite difference numerical solution

The set of coupled non-linear differential eqs. (10)-(13) subjected to the initial and boundary conditions (14) are solved by implicit finite difference scheme of Crank-Nicolson

Rashidi, M. M., *et al.*: Numerical Solution for Thermophoresis Effects on Heat and Mass ...
THERMAL SCIENCE: Year 2017, Vol. 21, No. 6B, pp. 2719-2730

2723

type. The discretized form of continuity, velocity, temperature, and concentration equations are given as:

$$\frac{U_{i,j}^{n+1} - U_{i-1,j}^{n+1} + U_{i,j}^{n} - U_{i-1,j}^{n}}{2\Delta X} + \frac{V_{i,j+1}^{n+1} - V_{i,j-1}^{n+1} + V_{i,j+1}^{n} - V_{i,j-1}^{n}}{4\Delta Y} = 0 \tag{17}$$

$$\frac{U_{i,j}^{n+1} - U_{i,j}^{n}}{\Delta t} + \frac{U_{i,j}^{n}\left(U_{i,j}^{n+1} - U_{i-1,j}^{n+1} + U_{i,j}^{n} - U_{i-1,j}^{n}\right)}{2\Delta X} + \frac{V_{i,j}^{n}\left(U_{i,j+1}^{n+1} - U_{i,j-1}^{n+1} + U_{i,j+1}^{n} - U_{i,j-1}^{n}\right)}{4\Delta Y} =$$
$$= \frac{U_{i,j-1}^{n+1} - 2U_{i,j}^{n+1} + U_{i,j+1}^{n+1} + U_{i,j-1}^{n} - 2U_{i,j}^{n} + U_{i,j+1}^{n}}{2\left(\Delta Y\right)^2} \tag{18}$$

$$\frac{\theta_{i,j}^{n+1} - \theta_{i,j}^{n}}{\Delta t} + \frac{U_{i,j}^{n}\left(\theta_{i,j}^{n+1} - \theta_{i-1,j}^{n+1} + \theta_{i,j}^{n} - \theta_{i-1,j}^{n}\right)}{2\Delta X} + \left[V_{i,j}^{n} - \frac{N}{\Pr}\frac{\left(\theta_{i,j+1}^{n+1} - \theta_{i,j-1}^{n+1} + \theta_{i,j+1}^{n} - \theta_{i,j-1}^{n}\right)}{4\Delta Y}\right] +$$
$$+ \frac{\left(\theta_{i,j+1}^{n+1} - \theta_{i,j-1}^{n+1} + \theta_{i,j+1}^{n} - \theta_{i,j-1}^{n}\right)}{4\Delta Y} = \frac{1}{\Pr}\left[1 + \frac{N}{2}\left(\theta_{i,j}^{n+1} + \theta_{i,j}^{n}\right)\right] +$$
$$+ \frac{\theta_{i,j-1}^{n+1} - 2\theta_{i,j}^{n+1} + \theta_{i,j+1}^{n+1} + \theta_{i,j-1}^{n} - 2\theta_{i,j}^{n} + \theta_{i,j+1}^{n}}{2\left(\Delta Y\right)^2} - \delta\left(\frac{U_{i,j}^{n+1} + U_{i,j}^{n}}{2}\right)\left(\frac{\theta_{i,j}^{n+1} + \theta_{i,j}^{n}}{2}\right) \tag{19}$$

$$\frac{\phi_{i,j}^{n+1} - \phi_{i,j}^{n}}{\Delta t} + \frac{U_{i,j}^{n}\left(\phi_{i,j}^{n+1} - \phi_{i-1,j}^{n+1} + \phi_{i,j}^{n} - \phi_{i-1,j}^{n}\right)}{2\Delta X} + \left(V_{i,j}^{n} + \tau_T\frac{\theta_{i,j+1}^{n+1} - \theta_{i,j-1}^{n+1} + \theta_{i,j+1}^{n} - \theta_{i,j-1}^{n}}{4\Delta Y}\right) +$$
$$+ \frac{\phi_{i,j+1}^{n+1} - \phi_{i,j-1}^{n+1} + \phi_{i,j+1}^{n} - \phi_{i,j-1}^{n}}{4\Delta Y} + \tau_T\left(\frac{\theta_{i,j-1}^{n+1} - 2\theta_{i,j}^{n+1} + \theta_{i,j+1}^{n+1} + \theta_{i,j-1}^{n} - 2\theta_{i,j}^{n} + \theta_{i,j+1}^{n}}{2\left(\Delta Y\right)^2}\right)\left(\frac{\phi_{i,j}^{n+1} + \phi_{i,j}^{n}}{2}\right) =$$
$$= \frac{1}{Sc}\frac{\phi_{i,j-1}^{n+1} - 2\phi_{i,j}^{n+1} + \phi_{i,j+1}^{n+1} + \phi_{i,j-1}^{n} - 2\phi_{i,j}^{n} + \phi_{i,j+1}^{n}}{2\left(\Delta Y\right)^2} \tag{20}$$

Here the subscript i designates the grid-point with X- co-ordinate $\sum_{i=0}^{I}\Delta X_i$, subscript j designates the grid-point with Y- co-ordinate $\sum_{j=0}^{J}\Delta Y_j$ and the superscript n designates a value of time $t = n\Delta t$. We consider a rectangular region with X varying from 0 to 1 and Y varying from 0 to 22, where Y_{max} is regarded as $Y \to \infty$. It is ensured that Y_{max} lies well outside the dynamic, thermal and mass diffusion boundary-layers. The mesh spacing in the X- and Y-directions $\Delta X = 0.05$, $\Delta Y = 0.05$ and time interval $\Delta t = 0.01$ are selected to obtain the tolerance limit within 10^{-5}. Computations are repeated until the steady-state is reached. A convergence criterion based on the relative difference between the two consecutive iteration values is employed. When the difference reaches less than 10^{-5} at all grid points, the solution is assumed to have converged and the iterative process is terminated. The scheme is unconditionally stable. The local truncation error is $O(\Delta t^2 + \Delta X^2 + \Delta Y^2)$ and it tends to zero as Δt, ΔX, and ΔY tend to zero. It follows that the Crank-Nicolson method is compatible. Stability and compatibility ensure the convergence.

Result and discussion

This section provides a manifestation of numerical calculations for various governing parameters on the velocity, temperature, concentration, skin friction, Nusselt number, and Sherwood number distributions which are illustrated in form of figs. 2-15. Based on the previous investigations, the governing parameters are fastened with following default parametric values: $t = 15$, $Pr = 2.97$, $\delta = 1$, $N = 2$, $\tau_T = 0.5$, $Sc = 0.96$, and $U_P = 0.5$, unless specifically indicated on the appropriate graph. For this set of fixed values, the velocity, temperature and concentration distributions of the plate reach the steady-state solution when time $t = 9.05$, 8.01, and 6.91, respectively. Thus, in all the computations $t = 15$ is fixed.

Figure 2 illustrates that an increase in velocity of the moving plate has the tendency to increase the fluid velocity. It is evident from fig. 3 that an increase in Prandtl number used to decrease the thermal conductivity of the fluid in the boundary-layer as well as the thermal boundary-layer thickness which decrease the fluid temperature. Figure 4 shows the graphical representation of the temperature profiles for different values of heat source/sink parameter. It is to be noted that negative values of δ indicate heat generation while positive values of δ correspond to heat absorption. It is observed that the boundary-layer generates the energy resulting in the temperature increases with increasing values of $\delta < 0$ (heat source) whereas in the case $\delta > 0$, boundary-layer absorbs the energy, which causes the temperature profiles to decrease considerably with increasing the values of $\delta > 0$ (heat sink). Typical variations of the temperature profiles in the presences of heat sink are shown in fig. 5 for various values of variable thermal conductivity of the fluid. The results show that an increase in the variable thermal conductivity parameter increases the temperature profiles.
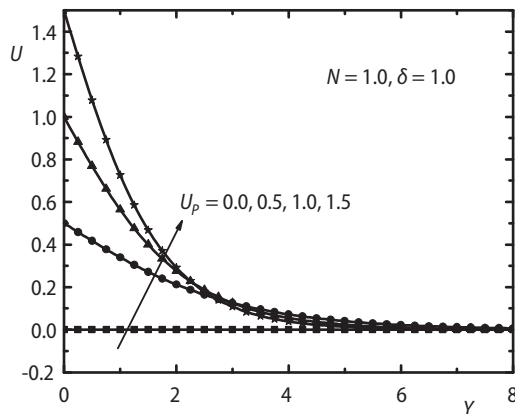

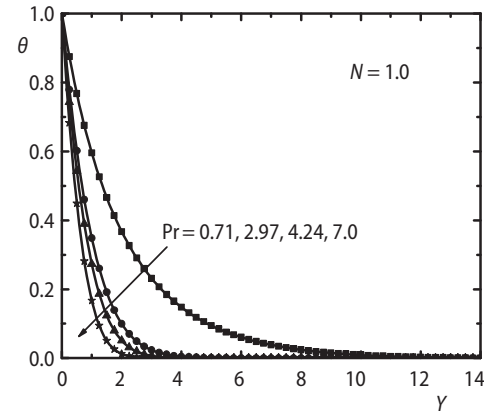**Figure 2. Velocity profiles for different values of U_P**

Figure 3. Temperature profiles for different values of Prandtl number

It is observed from fig. 6 that the mass transfer is diminished for increasing the values of Schmidt number. Physically it is true, since the higher values of Schmidt number have the tendency to dilute molecular diffusivity and therefore decrease in thickness of the concentration boundary-layer. The values of the Schmidt number are chosen to represent the presence of species by hydrogen (0.22), water vapor (0.6), CO_2 (0.96), and hydrocarbon derivatives (2). The fluid concentration decreases for increasing the thermophoretic parameter as shown in fig. 7. It is to be noted that concentration of the fluid gradually changes from higher value to the lower value only when the strength of the thermophoresis particle deposition is higher than the temperature-dependent fluid viscosity strength.
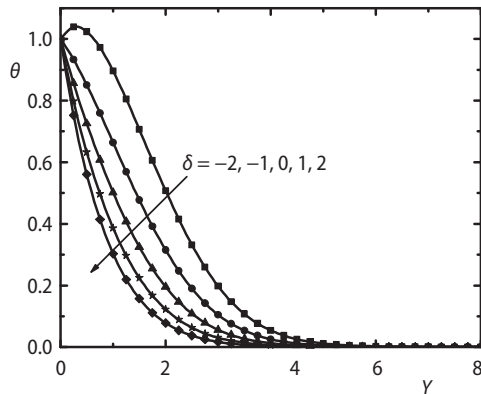
Rashidi, M. M., *et al.*: Numerical Solution for Thermophoresis Effects on Heat and Mass ...
THERMAL SCIENCE: Year 2017, Vol. 21, No. 6B, pp. 2719-2730

2725

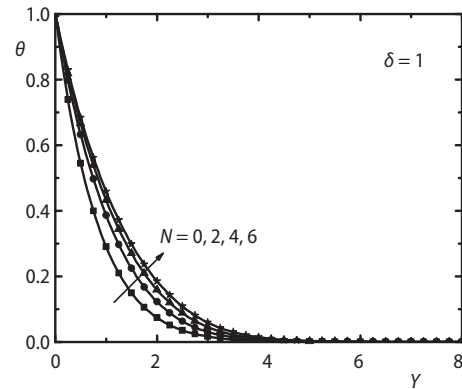**Figure 4. Temperature profiles for different values of δ**

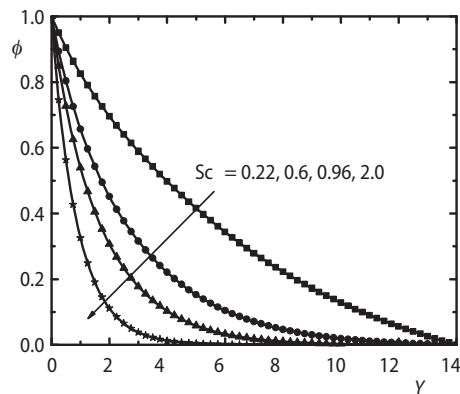**Figure 5. Temperature profiles for different values of N**

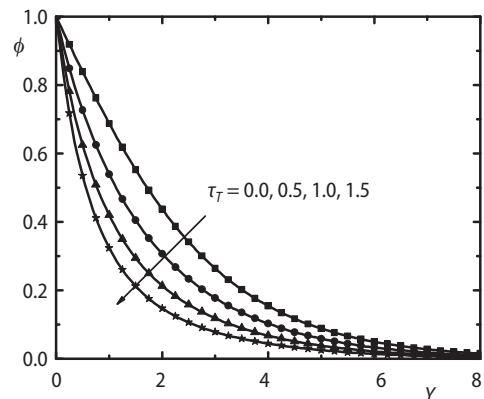**Figure 6. Concentration profiles for different values of Schmidt number**

Figure 7. Concentration profiles for different values of τ_T

Figure 8 shows the effects of U_P on local skin friction against the stream-wise co-ordinate X. It is observed that the local skin friction increases for increasing the velocity of the moving plate. The influence of δ, Pr, and N on the local Nusselt number for heat sink/source against the stream-wise co-ordinate X is illustrated in fig. 9-12. It is apparent from fig. 9 that the rate of heat transfer increases for diluting the strength of heat sink ($\delta > 0$) whereas it decreases for amplifying the heat source ($\delta < 0$). Figures 10 and 11 depict an increase in the Prandtl number increases the local Nusselt number for both heat sink and source. It is clear from fig. 12 that the Nusselt number decreases for increasing the variable thermal conductivity parameter in the presence of heat sink. Figures 13-15 depict the variation of surface concentration gradient against the stream-wise co-ordinate X for different values of Sc and τ_T in the presence of heat sink/source. Figure 13 elucidates that the local Sherwood number profiles increase for increasing the value of the Schmidt number. It is observed form figs. 14 and 15 that the local Sherwood number increases for increasing thermophoretic parameter in the presence of both heat sink and source. Table 1 shows the effects of t, U_P, δ, N, and τ_T on average skin friction, average Nusselt number and average Sherwood number distributions in the moving plate.

2726

Rashidi, M. M., *et al.*: Numerical Solution for Thermophoresis Effects on Heat and Mass ...
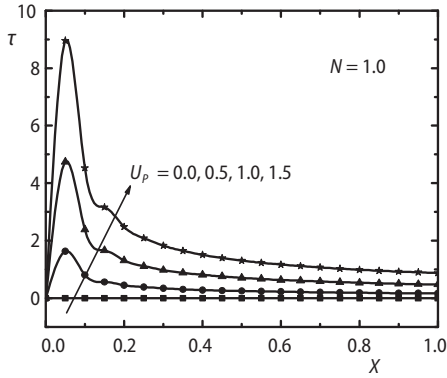THERMAL SCIENCE: Year 2017, Vol. 21, No. 6B, pp. 2719-2730

Figure 8. Local skin friction profiles for different values of U_P
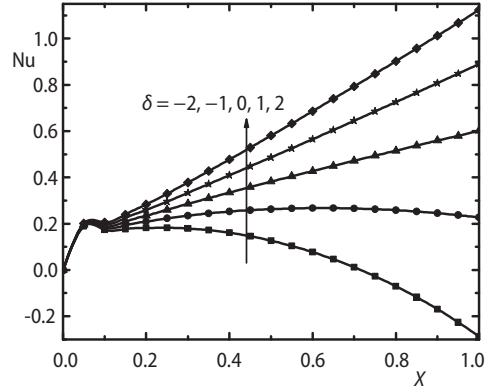

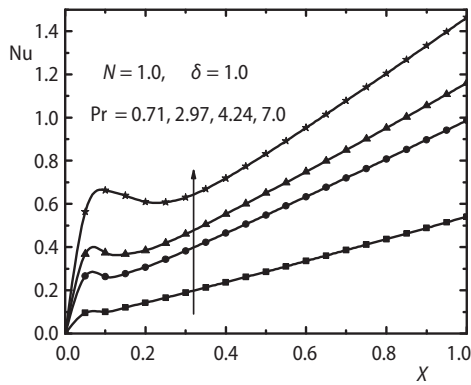**Figure 9. Local Nusselt number profiles for different values of δ**

Figure 10. Local Nusselt number profiles for different values of Prandtl number in the presence $\delta > 0$
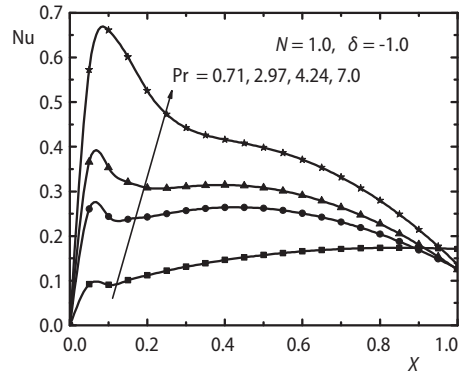

Figure 11. Local Nusselt number profiles for different values of Prandtl number in the presence $\delta < 0$
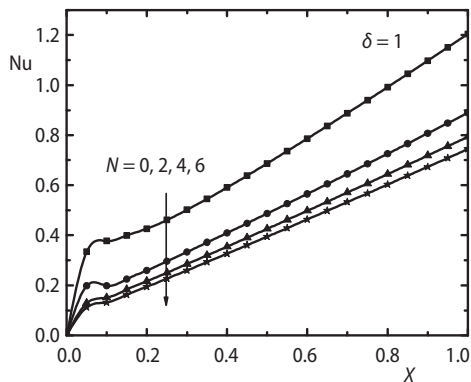

Figure 12. Local Nusselt number profiles for different values of N in the presence $\delta > 0$
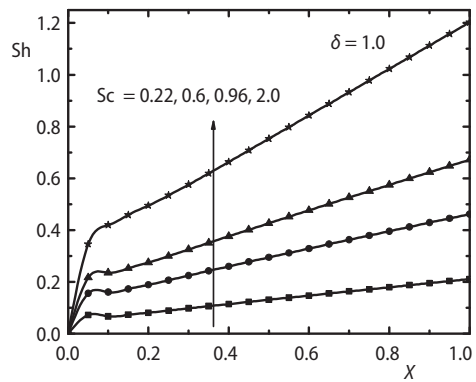

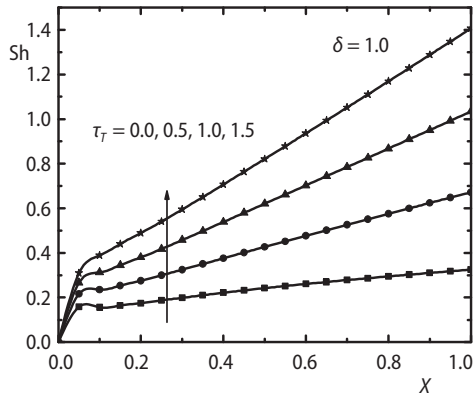**Figure 13. Local Sherwood number profiles for different values of Schmidt number in the presence $\delta > 0$**

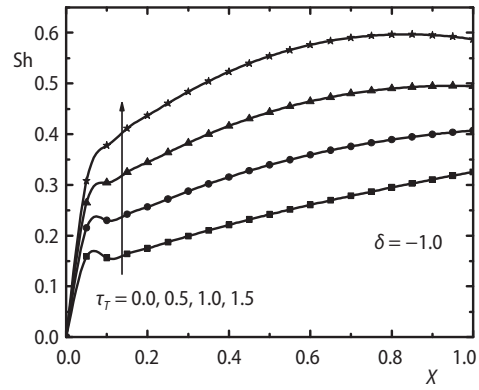**Figure 14. Local Sherwood number profiles for different values of τ_T in the presence $\delta > 0$**

Figure 15. Local Sherwood number profiles for different values of τ_T in the presence $\delta < 0$

Table 1. Effect of t, U_P, δ, N, and τ_T on $\overline{\tau}$, $\overline{Nu}$, and $\overline{Sh}$

Physical parameters	Values	Heat sink			Heat source		
		$\overline{\tau}$	$\overline{Nu}$	$\overline{Sh}$	$\overline{\tau}$	$\overline{Nu}$	$\overline{Sh}$
t	0	–3.06536	7.16296	6.37419	–3.06536	7.16296	6.37419
	1	–0.42858	1.27327	1.28213	–0.42858	0.94807	1.15888
	2	–0.38988	1.24140	1.20487	–0.38988	0.84488	1.05215
U_P	0	–0.00001	0.35871	0.27951	–0.00001	0.35833	0.27935
	0.5	–0.38083	1.48831	1.26980	–0.38083	0.95330	1.06111
	1	–1.0992	2.25855	1.77572	–1.09923	1.53572	1.50694
δ	–1	–0.38083	0.82710	1.03288	–0.38083	0.82710	1.03288
	0	–0.38083	1.05286	1.11907	–0.38083	1.05286	1.11907
	1	–0.38083	1.24613	1.19394	–0.38083	1.24613	1.19394
N	0	–0.38083	1.91450	1.41358	–0.38083	1.12749	1.10175
	2	–0.38083	1.24613	1.19394	–0.38083	0.82710	1.03288
	4	–0.38083	1.01224	1.11533	–0.38083	0.71251	1.00161
τ_T	0	–0.38083	1.24613	0.74079	–0.38083	0.82710	0.74079
	0.5	–0.38083	1.24613	1.19394	–0.38083	0.82710	1.03288
	1	–0.38083	1.24613	1.65164	–0.38083	0.82710	1.32729

Conclusions

The objective of this paper is to examine the influence of heat sink/source, variable thermal conductivity and thermophoretic particle deposition on free convective flow of a viscous fluid over a moving plate. The Crank-Nicolson method is used to solve the problem and the results are evaluated numerically and displayed graphically. The main findings of this investigation are summarized as follows.

- Velocity profiles increase for increasing the velocity of the moving plate.
- The heat transfer enhances with an increase in the heat source values ($\delta < 0$) whereas it decreases for increasing the values of heat sink ($\delta > 0$).

- The fluid temperature decreases for higher values of Prandtl number whereas it enhances for increasing the variable thermal conductivity parameter.
- Concentration profiles decrease for increasing the value of Schmidt number and thermophoretic parameter.
- It is observed from the local Nusselt number and Sherwood number distributions that the influence of heat source is more pronounced for lower values of X ($X < 0.5$) whereas the heat sink has more pronounced effect for higher values of X ($X > 0.5$).

Nomenclature

C – species concentration, [$\mathrm{mol\,m^{-3}}$]
C_i – constants ($i = 1, 2, 3, s, m, t$)
C_w – wall concentration, [$\mathrm{mol\,m^{-3}}$]
C_∞ – ambient concentration, [$\mathrm{mol\,m^{-3}}$]
c_p – specific heat at constant pressure, [$\mathrm{Jkg^{-1}K^{-1}}$]
D – molecular diffusivity, [$\mathrm{m^2s^{-1}}$]
Gr – thermal Grashof number, [–]
g – gravity, [$\mathrm{ms^{-2}}$]
Kn – Knudsen number, [–]
k_f – thermal conductivity, [$\mathrm{Wm^{-1}K^{-1}}$]
k_p – thermal conductivity of diffused particles, [$\mathrm{Wm^{-1}K^{-1}}$]
k_0 – coefficient of thermal conductivity, [$\mathrm{Wm^{-1}K^{-1}}$]
L – length, [m]
N – variable thermal conductivity of the fluid
Nu – local Nusselt number, [–]
$\overline{\mathrm{Nu}}$ – average Nusselt number, [–]
Pr – Prandtl number, [–]
Sc – Schmidt number, [–]
Sh – local Sherwood number, [–]
$\overline{\mathrm{Sh}}$ – average Sherwood number, [–]
T – fluid temperature, [K]

T_r – reference temperature, [K]
T_w – wall temperature, [K]
T_∞ – ambient temperature, [K]
t^* – dimensional time, [s]
U_p – velocity of the moving plate, [$\mathrm{ms^{-1}}$]
u – component of dimensional velocity along x-direction, [$\mathrm{ms^{-1}}$]
u_p – dimensional velocity of the moving plate, [$\mathrm{ms^{-1}}$]
v – component of dimensional velocity along, y-direction, [$\mathrm{ms^{-1}}$]

Greek symbols

β – constant
δ – non-dimensional longitudinal co-ordinate
θ – dimensionless temperature
μ – dynamic viscosity, [$\mathrm{kgm^{-1}s^{-1}}$]
ν – kinematic viscosity, [$\mathrm{m^2s^{-1}}$]
ρ – density, [$\mathrm{kgm^{-3}}$]
τ – local skin-friction
$\overline{\tau}$ – average skin friction
τ_T – thermophoretic parameter
ϕ – variables

References

[1] Mukhopadhyay, S., *et al.*, Steady Boundary Layer Flow and Heat Transfer over a Porous Moving Plate in Presence of Thermal Radiation, *International Journal of Heat and Mass Transfer*, *54* (2011), 13-14, pp. 2751-2757
[2] Rashidi, M. M., Erfani, E., The Modified Differential Transform Method for Investigating Nano Boundary-Layers over Stretching Surfaces, *International Journal of Numerical Methods for Heat and Fluid Flow*, *21* (2011), 7, pp. 864-883
[3] Rushi Kumar, B., Sivaraj, R., Heat and Mass Transfer in MHD Viscoelastic Fluid Flow over a Vertical Cone and Flat Plate with Variable Viscosity, *International Journal of Heat and Mass Transfer*, *56* (2013), 1-2, pp. 370-379
[4] Nandkeolyar, R., *et al.*, Unsteady Hydromagnetic Natural Convection Flow of a Dusty Fluid Past an Impulsively Moving Vertical Plate with Ramped Temperature in the Presence of Thermal Radiation, *ASME-Journal of Applied Mechanics*, *80* (2013), 6, pp. 1-9
[5] Rashidi, M. M., *et al.*, Free Convective Heat and Mass Transfer for MHD Fluid Flow over a Permeable Vertical Stretching Sheet in the Presence of the Radiation and Buoyancy Effects, *Ain Shams Engineering Journal*, *5* (2014), 3, pp. 901-912
[6] Singh, G., Makinde, O. D., Mixed Convection Slip Flow with Temperature Jump along a Moving Plate in Presence of Free Stream, *Thermal Science*, *19* (2015), 1, pp. 119-128
[7] Slattery, J. C., *Momentum Energy and Mass Transfer in Continua*, McGraw Hill, New York, USA, 1972
[8] Saravanan, S., Kandaswamy, P., Low Prandtl Number Magneto Convection in Cavities: Effect of Variable Thermal Conductivity, *ZAMM*, *80* (2000), 8, pp. 570-576

[9]   Talukdar, P., Mishra, S. C., Transient Conduction and Radiation Heat Transfer with Variable Thermal
      Conductivity, *Numerical Heat Transfer A*, *41* (2002), 8, pp. 851-867
[10] Seddeek, M. A., *et al.,* Numerical Study for the Effects of Thermophoresis and Variable Thermal Con-
      ductivity on Heat and Mass Transfer over an Accelerating Surface with Heat Source, *Computational
      Materials Science*, *47* (2009), 1, pp. 93-98
[11] Rashidi, M. M., *et al.,* Investigation of Entropy Generation in MHD and Slip Flow over a Rotating Porous
      Disk with Variable Properties, *International Journal of Heat and Mass Transfer*, *70* (2014), Mar., pp.
      892-917
[12] Acharya, M., *et al.,* Heat and Mass Transfer over an Accelerating Surface with Heat Source in Presence
      of Suction and Blowing, *International Journal of Engineering Science*, *37* (1999), 2, pp. 189-211
[13] Chamkha, A. J., Thermal Radiation and Buoyancy Effects on Hydromagnetic Flow over an Accelerating
      Permeable Surface with Heat Source or Sink, *International Journal of Engineering Science*, *38* (2000),
      15, pp. 1699-1712
[14] Makinde, O. D., Computational Modelling of MHD Unsteady Flow and Heat Transfer over a Flat Plate
      with Navier Slip and Newtonian Heating, *Brazilian Journal of Chemical Engineering, 29* (2012), 1, pp.
      159-166
[15] Makinde, O. D., Chemically Reacting Hydromagnetic Unsteady Flow of a Radiating Fluid Past a Vertical
      Plate with Constant Heat Flux, *Zeitschrift fuer Naturforschung, 67* (2012), 5, pp. 239-247
[16] Sivaraj, R., Rushi Kumar, B., Viscoelastic Fluid Flow over a Moving Vertical Cone and Flat Plate with
      Variable Electric Conductivity, *International Journal of Heat and Mass Transfer*, *61* (2013), June, pp.
      119-128
[17] Makinde, O. D., Tshehla M. S., Unsteady Hydromagnetic Flow of Radiating Fluid Past a Convectively
      Heated Vertical Plate with the Navier Slip, *Advances in Mathematical Physics, 2014* (2014), ID 973593
[18] Khan, W. A., *et al.*, Combined Heat and Mass Transfer of Third-Grade Nanofluids over a Convectively-
      -Heated Stretching Permeable Surface, *The Canadian Journal of Chemical Engineering, 93* (2015), 10,
      pp. 1880-1888
[19] Uddin, Z., *et al.,* Influence of Thermal Radiation and Heat Generation/Absorption on MHD Heat Transfer
      Flow of a Micropolar Fluid Past a Wedge with Hall and Ion Slip Currents, *Thermal Science*, *18* (2014),
      Suppl. 2, pp. S489-S502
[20] Talbot, L., *et al.*, Thermophoresis of Particles in a Heated Boundary Layer, *Journal of Fluid Mechanics*,
      101 (1980), 4, pp. 737-758
[21] Batchelor, G. K., Shen, C., Thermophoretic Deposition of Particles in Gas Flowing over Cold Surfaces,
      Journal of Colloid and Interface Science, *107* (1985), 1, pp. 21-37
[22] Rahman, M. M., Postelnicu, A., Effects of Thermophoresis on the Forced Convective Laminar Flow of a
      Viscous Incompressible Fluid over a Rotating Disk, *Mechanics Research Communications*, *37* (2010), 6,
      pp. 598-603
[23] Singh, N. P., *et al.*, Effects of Thermophoresis on Hydromagnetic Mixed Convection and Mass Transfer
      Flow Past a Vertical Permeable Plate with Variable Suction and Thermal Radiation, *Communication in
      Nonlinear Science and Numerical Simulation*, *16* (2011), 6, pp. 2519-2534
[24] Anika, N. N., *et al.*, Thermal Diffusion Effect on Unsteady Viscous MHD Micropolar Fluid Flow through
      an Infinite Plate with Hall and Ion-Slip Current, *Procedia Engineering*, *105* (2015), Dec., pp. 160-166
[25] Anika, N. N., *et al.*, Hall Current Effects on Magnetohydrodynamics Fluid over an Infinite Rotating
      Vertical Porous Plate Embedded in Unsteady Laminar Flow, *Annals of Pure and Applied Mathematics*, *3*
      (2013), 2, pp. 189-200
[26] Anika, N. N., Hoque, M. M., Thermal Buoyancy Force Effects on Developed Flow Considering Hall and
      Ion-Slip Current, *Annals of Pure and Applied Mathematics*, *3* (2013), 2, pp. 179-188
[27] Anika, N. N., *et al.*, Unsteady Free Convection Flow with Flow Control Parameter, *Current Trends in
      Technology and Science*, *2* (2013), 1, pp. 193-201
[28] Rashidi, M. M., *et al.,* Comparative Numerical Study of Single and Two-Phase Models of Nanofluid Heat
      Transfer in Wavy Channel, *Applied Mathematics and Mechanics* (English Edition), *35* (2014), 7, pp.
      831-848
[29] Rashidi, M. M., *et al.,* A Study on Heat Transfer in a Second-Grade Fluid through a Porous Medium with
      the Modified Differential Transform Method, *Heat Transfer – Asian Research, 42* (2013), 1, pp. 31-45
[30] Garoosi, F., *et al.*, Two-Phase Mixture Modeling of Mixed Convection of Nanofluids in a Square Cavity
      with Internal and External Heating, *Powder Technology, 275* (2015), May, pp. 304-321

[31] Garoosi, F., *et al.*, Numerical Simulation of Natural Convection of the Nanofluid in Heat Exchangers using a Buongiorno Model, *Applied Mathematics and Computation, 254* (2015), Mar., pp. 183-203

[32] Rashidi, M. M., *et al.,* Mixed Convective Heat Transfer for MHD Viscoelastic Fluid Flow over a Porous Wedge with Thermal Radiation, *Advances in Mechanical Engineering, 6* (2014), ID 735939